RAPID COMMUNICATION

Superconductivity in electron-doped arsenene*

Xin Kong(孔鑫)[1,2], Miao Gao(高淼)[3,†], Xun-Wang Yan(闫循旺)[4], Zhong-Yi Lu(卢仲毅)[5], and Tao Xiang(向涛)[1,6]

[1] *Institute of Physics, Chinese Academy of Sciences, Beijing* 100190, *China*
[2] *School of Physical Sciences, University of Chinese Academy of Sciences, Beijing* 100049, *China*
[3] *Department of Microelectronics Science and Engineering, Faculty of Science, Ningbo University, Ningbo* 315211, *China*
[4] *College of Physics and Engineering, Qufu Normal University, Qufu* 273165, *China*
[5] *Department of Physics, Renmin University of China, Beijing* 100872, *China*
[6] *Collaborative Innovation Center of Quantum Matter, Beijing* 100190, *China*

(Received 22 February 2018; revised manuscript received 2 March 2018; published online 29 March 2018)

Based on the first-principles density functional theory electronic structure calculation, we investigate the possible phonon-mediated superconductivity in arsenene, a two-dimensional buckled arsenic atomic sheet, under electron doping. We find that the strong superconducting pairing interaction results mainly from the p_z-like electrons of arsenic atoms and the A_1 phonon mode around the K point, and the superconducting transition temperature can be as high as 30.8 K in the arsenene with 0.2 doped electrons per unit cell and 12%-applied biaxial tensile strain. This transition temperature is about ten times higher than that in the bulk arsenic under high pressure. It is also the highest transition temperature that is predicted for electron-doped two-dimensional elemental superconductors, including graphene, silicene, phosphorene, and borophene.

Keywords: arsenene, phonon-mediated superconductivity, first-principles calculation, maximally localized Wannier functions

PACS: 63.20.kd, 74.20.Pq, 74.72.Ek, 74.78.–w **DOI:** 10.1088/1674-1056/27/4/046301

1. Introduction

Recently there has been a surge of interest in the investigation of two-dimensional (2D) superconductors, partially due to their potential application in nano-superconducting devices.[1,2] A pure 2D electronic system can be obtained by growing a single layer graphite or other materials on a proper substrate. The interplay between a 2D superconductor and the substrate has proven to be an efficient way to enhance superconductivity. For example, the superconducting transition temperature, T_c, of a single layer FeSe film deposited on the (001) surface of $SrTiO_3$ is greatly enhanced[3,4] in comparison with the bulk FeSe superconductor,[5] resulting from the coupling between electrons and the phonon modes in the substrate.[6]

Superconductivity in graphene, which is the first 2D compound synthesized at laboratory, was extensively explored. Through a plasmon-mediated mechanism, Uchoa *et al.* discussed properties of superconducting states in several metal coated graphenes.[7] First-principles density functional theory (DFT) calculations predicted that the monolayer LiC_6 and CaC_6 are phonon-mediated superconductors with T_c of 8.1 K and 1.4 K, respectively.[8] Later, the superconducting phase was observed experimentally below 7.4 K in a Li-intercalated graphite thin film[9] and 6 K in a Ca-decorated graphene.[10] Calculations of electron-phonon interactions suggested that T_c of graphene can reach 23.8 K or even 31.6 K upon heavy electron or hole doping under 16.5% biaxial tensile strain (BTS),[11] but experimental evidence for such high-T_c superconductivity in doped graphenes is still not available.

In recent years, several new 2D materials, like silicene, phosphorene, and borophene, were synthesized experimentally. Similar to graphene, phosphorene is obtained by mechanically exfoliating layered black phosphorus.[12] Silicene[13,14] and borophene[15,16] were epitaxially grown on Ag (111) surfaces. It was reported that there is a charge transfer from the Ag (111) substrate to silicene[17] or borophene.[16] Furthermore, the substrate imposes strain to these single-layer materials, due to the lattice mismatch.[16,18–20] These effects of the substrate should be taken into account in the investigation of superconducting properties in these materials.

The DFT calculation also showed that the superconducting transition temperature can reach 16.4 K in silicene upon electron doping of $n_{2D} = 3.51 \times 10^{14}$ cm^{-2} and 5%-BTS.[21] T_c of phosphorene was predicted to be 12.2 K under the doping of 2.6×10^{14} cm^{-2} and 8%-uniaxial tensile strain along

*Project supported by the National Key Research and Development Program of China (Grant No. 2017YFA0302901), the National Natural Science Foundation of China (Grant Nos. 11474331, 11404383, and 11474004), the Natural Science Foundation of Zhejiang Province, China (Grant No. LY17A040005), and the K. C. Wong Magna Fund in Ningbo University.

†Corresponding author. E-mail: gaomiao@nbu.edu.cn

© 2018 Chinese Physical Society and IOP Publishing Ltd

the armchair direction.[22] Applying 4%-BTS to phosphorene can further increase T_c to 16 K.[23]

Unlike silicene and phosphorene, borophene is intrinsically a metal.[16] A free-standing pristine borophene is predicted to superconduct around 20 K,[24,25] especially for the χ_3-type borophene whose T_c can be 24.7 K.[25] This is the highest superconducting transition temperature among predicted or observed 2D elemental superconductors without doping. Unfortunately, the charge transfer and tensile strain imposed by the Ag substrate suppress the superconducting order dramatically.[25,26]

Recently, a buckled single-layer honeycomb arsenic, i.e., arsenene, was proposed.[27,28] Unlike the semi-metallic bulk gray arsenic, arsenene is a semiconductor with an indirect energy gap of 2.49 eV. More importantly, arsenene undergoes an intriguing indirect-to-direct gap transition by applying a small BTS. This makes arsenene a promising candidate of transistor with high on/off ratios, optoelectronic device working under blue or UV light, and 2D crystal-based mechanical sensor.[27] Furthermore, it was predicted that arsenene has a higher electron mobility than that of MoS_2,[29] and can become a unique topological insulator under suitable BTS without considering any spin-orbit coupling.[30]

In this work, we employ the first-principles DFT and the Wannier interpolation technique to accurately determine the electron–phonon coupling (EPC) properties of electron-doped arsenenes. The phonon-mediated superconducting T_c is evaluated based on the McMillian–Allen–Dynes formula. Without applying BTS, 0.1 electrons/cell (hereafter *e*/cell) doping can already turn arsenene into a superconductor with a superconducting temperature above the liquid-helium temperature. T_c increases to 10 K at 0.3 *e*/cell doping (i.e., $n_{2D} = 2.76 \times 10^{14}$ cm^{-2}). Moreover, we find that the A_1 phonon mode at the K point contributes mostly to the EPC constant. From the electronic point of view, the p_z-like electronic orbitals of arsenic atoms couple strongly with phonons. By applying a BTS, the A_1 phonon mode is softened and the EPC matrix elements are enhanced. This enlarges both the EPC λ and the superconducting transition temperature. Under a 0.2 *e*/cell doping and 12% BTS, T_c of arsenene is predicted to be about 30.8 K. To the best of our knowledge, this is the highest T_c predicted for 2D elemental superconductors upon electron doping.

2. Computational approach

In the DFT-based electronic structure calculation, the plane wave basis method is adopted.[31] We calculate the Bloch states and the phonon perturbation potentials[33] using the local density approximation and the norm-conserving pseudopotentials.[32] The kinetic energy cut-off and the charge density cut-off are taken to be 80 Ry (1 Ry = 13.6056923(12) eV) and 320 Ry, respectively. A slab model is used to simulate arsenene, in which a 12-Å vacuum is added to avoid the interaction between the neighboring arsenic sheets along the c axis. Electron doping is simulated by adding electrons into the system with a compensating background of uniform positive charges. For each doping concentration, the atomic positions are relaxed but with fixed in-plane lattice constants which are obtained by optimizing the lattice structure of arsenene without doping.

The charge density is calculated on an unshifted mesh of $60\times60\times1$ points, with a Methfessel–Paxton smearing[34] of 0.02 Ry. The dynamical matrix and perturbation potential are calculated on a Γ-centered $12\times12\times1$ mesh, within the framework of density-functional perturbation theory.[35] Maximally localized Wannier functions[36,37] are constructed on a $12\times12\times1$ grid of the Brillouin zone, using ten random Gaussian functions as the initial guess. Fine electron ($600\times600\times1$) and phonon ($200\times200\times1$) grids are used to interpolate the EPC constant using the Wannier90 and EPW codes.[38–41] Dirac δ-functions for electrons and phonons are replaced by smearing functions with widths of 15 and 0.2 meV, respectively.

The EPC constant λ is determined by the summation of the momentum-dependent coupling constant $\lambda_{\boldsymbol{q}\nu}$ over the first Brillouin zone or the integration of the Eliashberg spectral function $\alpha^2F(\omega)$ in the frequency space,[42,43]

$$\lambda = \frac{1}{N_q}\sum_{\boldsymbol{q}\nu}\lambda_{\boldsymbol{q}\nu} = 2\int\frac{\alpha^2F(\omega)}{\omega}\mathrm{d}\omega, \tag{1}$$

in which N_q represents the total number of $\boldsymbol{q}$ points in the fine $\boldsymbol{q}$-mesh. The coupling constant $\lambda_{\boldsymbol{q}\nu}$ for mode ν at wavevector $\boldsymbol{q}$ is defined by,[42,43]

$$\lambda_{\boldsymbol{q}\nu} = \frac{2}{\hbar N(0)N_k}\sum_{ij\boldsymbol{k}}\frac{1}{\omega_{\boldsymbol{q}\nu}}|g^{ij}_{\boldsymbol{k},\boldsymbol{q}\nu}|^2\delta(\varepsilon^i_{\boldsymbol{q}})\delta(\varepsilon^j_{\boldsymbol{k}+q}). \tag{2}$$

Here $\omega_{\boldsymbol{q}\nu}$ is the phonon frequency and $g^{ij}_{\boldsymbol{k},\boldsymbol{q}\nu}$ is the probability amplitude for scattering an electron with a transfer of crystal momentum $\boldsymbol{q}$. (i,j) and ν denote the indices of energy bands and phonon modes, respectively. $\varepsilon^i_{\boldsymbol{q}}$ and $\varepsilon^j_{\boldsymbol{k}+q}$ are the eigenvalues of the Kohn–Sham orbitals with respect to the Fermi energy. $N(0)$ is the density of states (DOS) of electrons at the Fermi level. N_k is the total number of $\boldsymbol{k}$ points in the fine Brillouin-zone mesh. The Eliashberg spectral function is determined by,[42,43]

$$\alpha^2F(\omega) = \frac{1}{2}\sum_{\boldsymbol{q}\nu}\delta(\omega-\omega_{\boldsymbol{q}\nu})\lambda_{\boldsymbol{q}\nu}\omega_{\boldsymbol{q}\nu}. \tag{3}$$

We calculate the superconducting transition temperature using the McMillian–Allen–Dynes formula,[43]

$$T_c = f_1f_2\frac{\omega_{\log}}{1.2}\exp\left[\frac{-1.04(1+\lambda)}{\lambda(1-0.62\mu^*)-\mu^*}\right]. \tag{4}$$

In Eq. (4), f_1 and f_2 are the correction factors, which equal 1 when $\lambda < 1.3$, and

$$f_1 = [1+(\lambda/\Lambda_1)^{3/2}]^{1/3}, \quad (5)$$

$$f_2 = 1+\frac{(\sqrt{\langle\omega^2\rangle}/\omega_{\log}-1)\lambda^2}{\lambda^2+\Lambda_2^2} \quad (6)$$

when $\lambda \geq 1.3$. Here $\Lambda_1 = 2.46(1+3.8\mu^*)$, $\Lambda_2 = 1.82(1+6.3\mu^*)(\sqrt{\langle\omega^2\rangle}/\omega_{\log})$. The effective screened Coulomb repulsion constant μ^* is set to 0.1, and

$$\omega_{\log} = \exp\left[\frac{2}{\lambda}\int\frac{\mathrm{d}\omega}{\omega}\alpha^2F(\omega)\log\omega\right],$$

$$\langle\omega^2\rangle = \frac{2}{\lambda}\int \mathrm{d}\omega\alpha^2F(\omega)\omega.$$

3. Results and discussion

3.1. EPC in electron-doped arsenene

For a free standing arsenene without doping, we find that the optimized lattice constant is 3.5411 Å, in agreement with the result, 3.5408 Å, obtained by Zhang *et al.*[27] Our calculation shows that arsenene is semiconducting with an indirect band gap of 1.42 eV. The valence band maximum is at the Γ point, while the conduction band minimum is located on the line between Γ and M. Although the energy gap is underestimated in comparison with the HSE06-level result,[27] it does not affect our EPC results since the shapes of conduction band given by LDA and HSE06 are concordant.

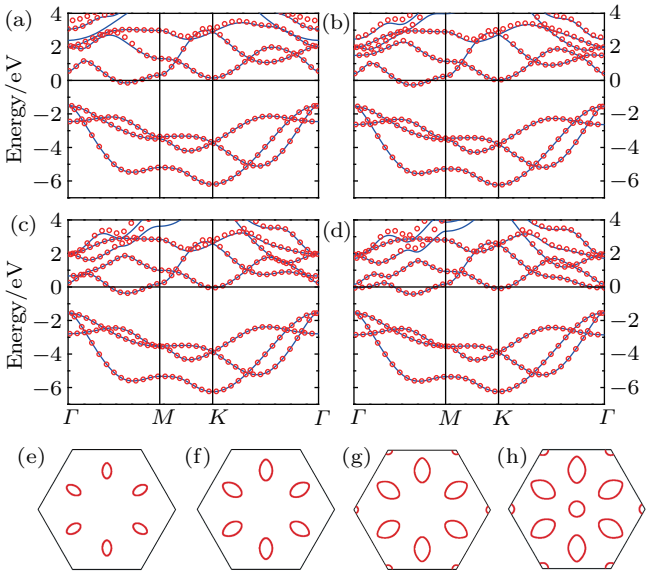


Fig. 1. (color online) Band structures of electron-doped arsenenes at four doping levels: (a) 0.1 *e*/cell, (b) 0.2 *e*/cell, (c) 0.3 *e*/cell, and (d) 0.4 *e*/cell. The Fermi energy is set to zero. The solid blue lines represent the band structures obtained by first-principles DFT calculations. The red circles denote the band structures obtained by interpolation with MLWFs. (e)–(h) Fermi surfaces correspond to the band structures shown in panels (a)–(d), respectively.

Figure 1 shows the band structures with the corresponding Fermi surfaces for four electron-doped arsenenes. At the doping of 0.1 *e*/cell, there are six elliptical electron pockets surrounding Γ. With the increase of the doping level, the area enclosed by each pocket expands. Moreover, six small electron arcs emerge at the Fermi level around the six zone corners when the doping level reaches 0.3 *e*/cell or above [Fig. 1(g)]. At higher doping, an electron pocket centred at the Γ point appears at the Fermi level [Fig. 1(h)]. The influence of electron doping on fully occupied energy bands is negligible.

Figure 2 shows the phonon spectra of electron-doped arsenenes. At the doping of 0.1 *e*/cell, there is no imaginary phonon frequency, indicating that this system is dynamically stable. Moreover, there is a gap between the acoustic and optical phonon modes. With the increase of doping, the optical phonon modes are gradually softened. At higher doping, imaginary frequencies are found in the lowest acoustic band near the Γ point [Figs. 2(b)–2(d)]. This kind of imaginary frequencies were also found in the phonon spectra of borophene,[25] arsenene,[28,30] germanene,[44] and other binary monolayer honeycomb materials.[45] It is not a sign of structure instability. Instead, it results from the numerical instability in the accurate calculation of rapidly decreasing interatomic forces.[45] The largest contribution to λ comes from the A_1 mode in the lowest optical phonon mode around the K point. A real-space picture of the eigen-vector of this mode is shown in Fig. 2(e) and Fig. 2(f).

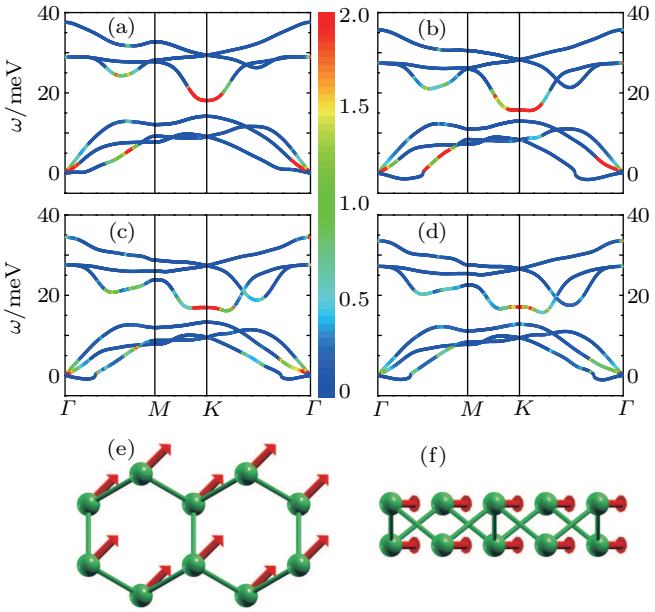


Fig. 2. (color online) Phonon spectra of electron-doped arsenenes at four doping levels: (a) 0.1 *e*/cell. (b) 0.2 *e*/cell. (c) 0.3 *e*/cell. (d) 0.4 *e*/cell. The amplitude of the EPC constant, i.e., λ_{qv} is mapped by different colors. Panels (e) and (f) show the top and side views of the A_1 optical phonon mode in real space.

The Eliashberg spectral function $\alpha^2F(\omega)$ shows two main peaks [Fig. 3]. The lower-frequency peak results from the A_1 phonon mode around the K point. In comparison with the peak at the 0.1 *e*/cell doping, the peak position shifts towards lower frequency at higher doping. The higher-frequency

peak is also mainly the contribution of the lowest optical phonon excitations, especially those between Γ and M. Even though the EPC $\lambda_{q\nu}$ of these phonons along Γ–M is smaller than that of the A_1 mode at the K point, the density of states is higher.

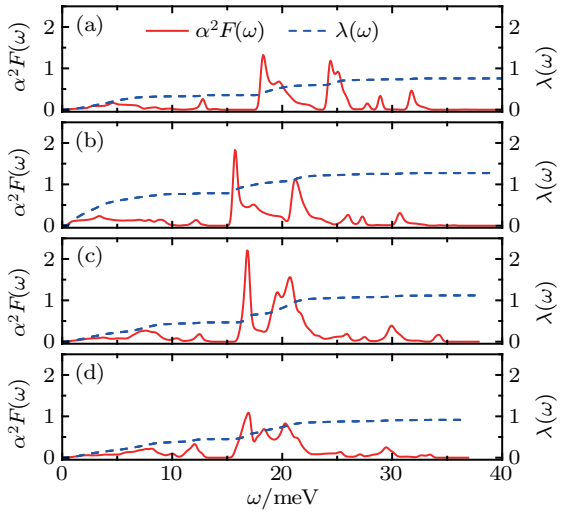


Fig. 3. (color online) Frequency dependence of the Eliashberg spectral function $\alpha^2F(\omega)$ and $\lambda(\omega)$ for four electron-doped arsenenes: (a) 0.1 e/cell. (b) 0.2 e/cell. (c) 0.3 e/cell. (d) 0.4 e/cell. $\lambda(\omega)$ is defined by $2\int_0^{\omega}(1/\omega')\alpha^2F(\omega')\mathrm{d}\omega'$.

Table 1. Predicted superconducting transition temperature T_c and other parameters obtained by the first-principles calculation at various doping (e/cell) and BTS ε (%): $N(0)$, frequency of A_1 phonon $\omega(A_1)$ (meV), λ, $\omega_{\log}$ (meV), $\sqrt{\langle\omega^2\rangle}$ (meV), and T_c (K).

Doping	ε	$N(0)$	$\omega(A_1)$	λ	$\omega_{\log}$	$\sqrt{\langle\omega^2\rangle}$	T_c
0.1	0.0	0.37	18.08	0.76	9.81	16.85	4.7
0.2	0.0	0.40	15.72	1.27	5.65	12.85	6.3
0.3	0.0	0.61	16.93	1.12	10.66	16.21	10.1
0.4	0.0	0.91	17.08	0.91	9.86	15.16	6.9
0.2	2.0	0.45	14.89	1.45	6.46	12.94	9.7
0.2	4.0	0.54	11.18	1.90	6.57	11.85	13.6
0.2	6.0	0.64	7.83	2.77	6.88	10.40	19.6
0.2	8.0	0.77	6.06	4.27	5.99	8.86	24.4
0.2	12.0	1.16	7.85	6.12	5.41	8.53	30.8

Based on the above results, we calculate the superconducting transition temperature T_c using the McMillian–Allen–Dynes formula.[43] The results, together with other key parameters, are presented in Table 1. Without BTS, T_c shows a maximum at 0.3 e/cell. λ at 0.2 e/cell is larger than that at 0.3 e/cell due to the considerable contribution from the acoustic phonon modes at the former doping [Fig. 2(b)], but the corresponding T_c is lower than the latter case.

The EPC constant λ is determined by the DOS, the phonon frequency $\omega_{q\nu}$, the EPC matrix element $|g^{ij}_{k,q\nu}|$, and other parameters. In order to determine which effect has the largest contribution to λ, we calculate the following two quantities

$$\xi(q) = \frac{1}{N(0)N_k}\sum_{ijk}\delta(\varepsilon^i_k)\delta(\varepsilon^j_{k+q}), \tag{7}$$

$$\gamma(q) = \frac{1}{N(0)N_k}\sum_{ij\nu k}|g^{ij}_{k,q\nu}|^2\delta(\varepsilon^i_q)\delta(\varepsilon^j_{k+q}). \tag{8}$$

$\xi(q)$ is a modified Fermi surface nesting function, in which $N(0)$ is also included. $\gamma(q)$ is the nesting function weighted by the EPC matrix element $|g^{ij}_{k,q\nu}|$.

Figure 4 shows $\xi(q)$, $\gamma(q)$, and $\lambda(q)$ (calculated through $\sum_\nu\lambda_{q\nu}$) for the four electron-doped arsenenes. At each doping level, the similarity between $\xi(q)$ and $\lambda(q)$ indicates that the strong EPC of the A_1 phonon mode mainly comes from the peak in the nesting function $\xi(q)$ around the K point. The relatively lower vibrational frequencies of strongly coupled phonon modes at the 0.2 e/cell doping lead to the sharp peaks between Γ and M and the largest λ. $\lambda(q)$ at 0.1 e/cell is comparable to that at 0.2 e/cell [Fig. 4(c)]. However, λ is a summation over the whole Brillouin zone. For the cases of 0.2, 0.3, and 0.4 e/cell doping, there is a certain amount of q points which have substantial contribution to $\lambda(q)$ [Fig. 4(d) and Fig. 4(e)] but are not located along the Γ–M–K–Γ high-symmetry line.

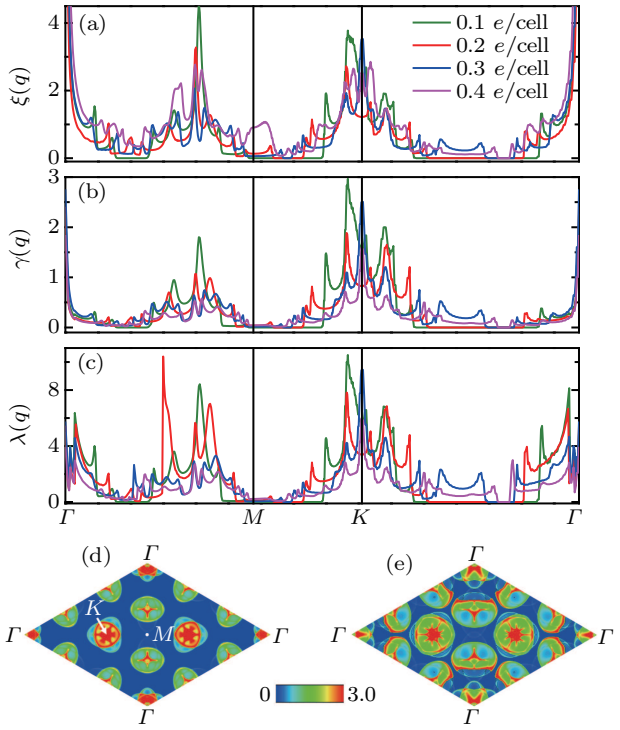


Fig. 4. (color online) Modified Fermi surface nesting function $\xi(q)$ (a), $\gamma(q)$ (b), and $\lambda(q)$ (c) of electron-doped arsenenes. Panels (d) and (e) represent the $\lambda(q)$ in the whole Brillouin zone for 0.1 e/cell and 0.2 e/cell doping, respectively. It is noted that the reciprocal unit cell instead of the first Brillouin zone is used.

3.2. EPC under BTS

The BTS is measured by $\varepsilon = (a - a_0)/a_0 \times 100\%$, where a_0 and a are the lattice constants without and with strain, respectively. Without doping, arsenene remains in the semiconducting phase under BTS up to 12%.[27] In order to study the BTS effect on the superconducting properties, we calculate the EPC of biaxial strained arsenenes under 0.2 e/cell doping.

At 4% BTS, as shown in Fig. 5(b), the conduction band minimum moves to the Γ point. This leads to a direct band gap of 1.67 eV, resembling the indirect-to-direct band-gap transition in the undoped arsenene under 4% BTS.[27] With the increase of BTS, the conduction band along the Γ–M line becomes less dispersive [Figs. 5(c)–5(d)], which enlarges the DOS at the Fermi level [see Table 1]. Furthermore, the applied BTS lowers the conducton-band energy at the Γ point, which enables an electron pocket around the Γ point to emerge at the Fermi surface and reduces the volume of the six elliptical Fermi surface sheets.

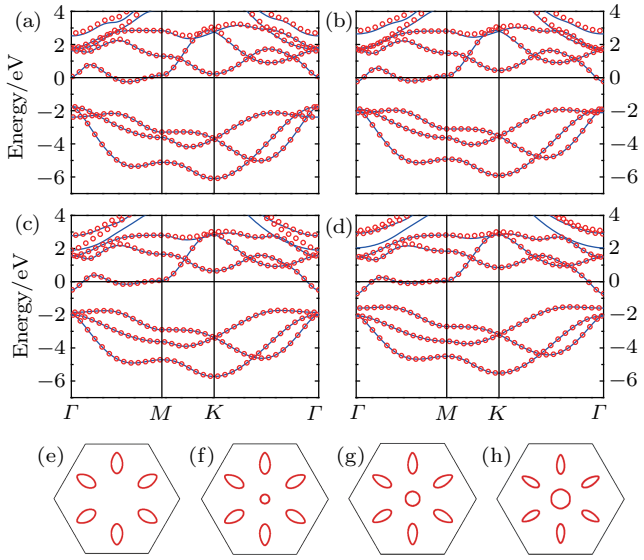


Fig. 5. (color online) Band structures of arsenenes with 0.2 *e*/cell electron doping under (a) 2%, (b) 4%, (c) 6%, and (d) 8% BTS. (e)–(h) The Fermi surfaces correspond to the band structures shown in panels (a)–(d), respectively.

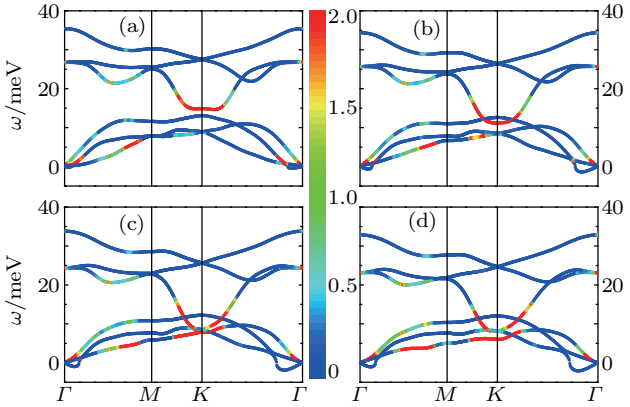


Fig. 6. (color online) Phonon spectra of arsenenes under (a) 2%, (b) 4%, (c) 6%, and (d) 8% BTS. The amplitude of λ_{qv} is mapped by different colors.

Figure 6 shows the phonon spectra of strained arsenenes. By applying the BTS, the phonon frequencies are softened, especially for the A_1 phonon mode around the K point. Meanwhile, the EPC from the lowest acoustic phonon band between the Γ and M points becomes stronger and stronger with the increase of BTS. Again, the phonon frequency in the lowest phonon band becomes imaginary around the Γ point. Further calculation, however, suggests that the 0.2 *e*/cell doped arsenene remains dynamically stable under 14% BTS, slightly smaller than the critical strain, 18.4%, as obtained in the undoped arsenene.[30]

When the applied BTS is less than 4%, the two-peak structures of $\alpha^2F(\omega)$ are preserved [Fig. 7(a) and Fig. 7(b)]. With the increase of BTS, $\alpha^2F(\omega)$ around 5 meV is enhanced. This enhancement arises from the softening of the A_1 mode and the enhancement of the EPC in the lowest acoustic phonon band between Γ and M. We also calculate $\xi(q)$, $\gamma(q)$, and $\lambda(q)$ for arsenene at different BTS [Fig. 8]. Similar to the case of the BTS-free arsenene, $\xi(q)$ is not a hegemonic factor that determines λ. In contrast, an obvious separation among the four curves in $\gamma(q)$ is observed. This separation results from the matrix element $|g^{ij}_{k,qv}|$ around the Fermi level [Fig. 8(b)]. It is further enhanced by the softening of strongly coupled phonon modes [Fig. 8(c)], giving rise to a T_c as high as 30.8 K at 8% BTS.

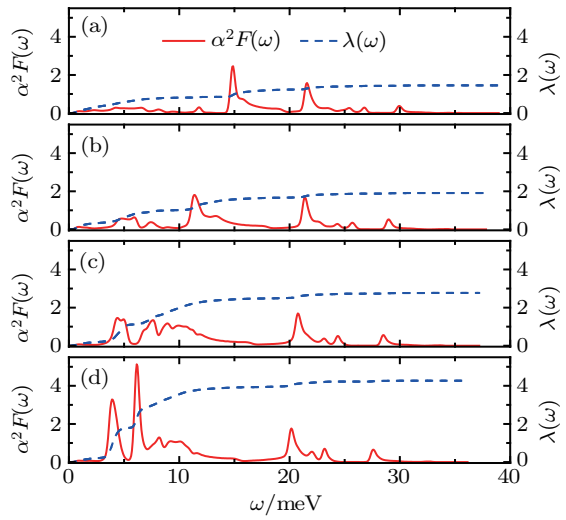


Fig. 7. (color online) Eliashberg spectral function $\alpha^2F(\omega)$ and $\lambda(\omega)$ the strained arsenenes with (a) 2%, (b) 4%, (c) 6%, and (d) 8% BTS.

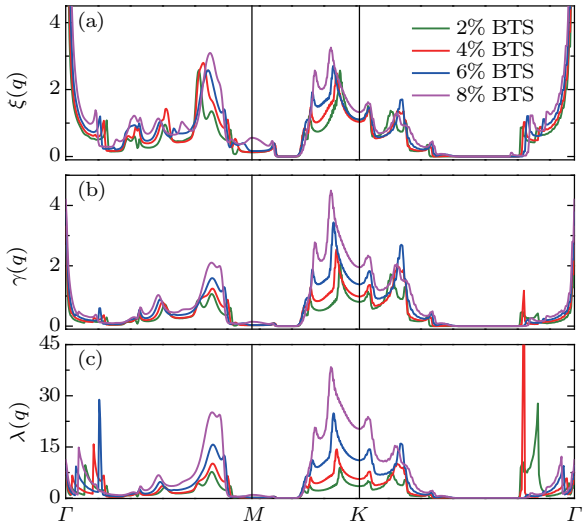


Fig. 8. (color online) $\xi(q)$, $\gamma(q)$, and $\lambda(q)$ of strained arsenenes.

To determine which electron band contributes most to the EPC, we calculate λ_{ki} defined by

$$\lambda_{ki} = \frac{2}{\hbar N(0) N_q} \sum_{q\nu j} \frac{1}{\omega_{q\nu}} |g^{ij}_{k,q\nu}|^2 \delta(\varepsilon^i_k) \delta(\varepsilon^j_{k+q}), \qquad (9)$$

where i is the band index of electrons. λ_{ki} describes the scattering process of an electron from the i-th band to other bands by a phonon with momentum q and branch ν. It represents the contribution of electrons with momentum k at the i-th band to the EPC.

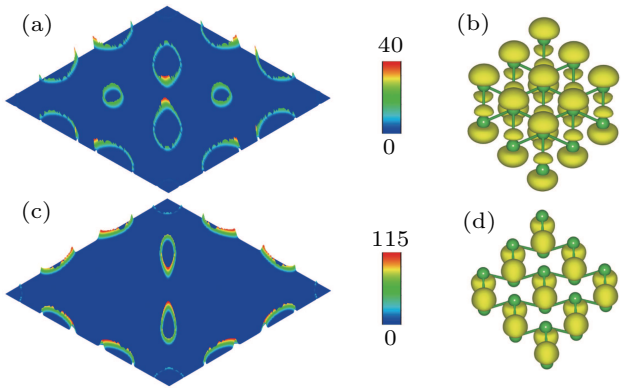


Fig. 9. (color online) (a) and (c): Three-dimensional views of λ_{ki} in the reciprocal unit cell. Panels (b) and (d): charge densities of electrons that couple most strongly with phonons. Panels (a) and (b) correspond to 0.4 e/cell doping without BTS. Panels (c) and (d) correspond to 0.2 e/cell doping with 8% BTS.

For all the cases we have studied, we find that λ_{ki} behaves similarly. Here we only show the results for the 0.4 e/cell doping without BTS [Fig. 9(a)] and for the 0.2 e/cell doping with 8% BTS [Fig. 9(c)]. By comparing the contour picture of λ_{ki} with the Fermi surface shape shown in Fig. 1(h) and Fig. 5(h), we find that the main contribution to the EPC comes from the elliptical Fermi surface sheets. In particular, the points near M contribute most to the EPC. The charge density of these electrons shows a p_z-like character [Fig. 9(b) and Fig. 9(d)], indicating that it is the p_z orbital of arsenic atom that couples most strongly with phonons.

The maximal superconducting T_c of 23.8 K is predicted for 4.65×10^{14} cm^{-2} electron-doped graphene under 16.5% BTS. Realistically, realizing such requirements in graphene may be very difficult in experiment. The advantage in the case of arsenene is that the high-T_c superconductivity above 30 K may be obtained under a relatively smaller doping density (1.28×10^{14} cm^{-2}) and BTS (12%). Recently, multilayer arsenenes were successfully grown on InAs using the plasma-assisted process.[46] The bulk gray arsenic, which is the most stable phase among all arsenic allotropes,[47] could be used as a precursor to prepare arsenene.[27,28] By growing arsenene on a piezoelectric substrate, one can control BTS by applying a bias voltage to elongate or shorten the lattice constants.[19] The electron doping can be achieved either by chemical doping or substitution, or by liquid or solid gating.[48,49] Thus it is feasible to verify our prediction experimentally.

4. Conclusion

Based on the first-principles DFT electronic structure calculation, we predict that the semiconducting arsenene can become a phonon-mediated superconductor upon doping of electrons. The maximal superconducting transition temperature is found to be around 10 K in the doped arsenene. It can be further lifted to 30 K by applying a 12% BTS. The superconducting pairing results mainly from the A_1 phonon mode around the K point and the p_z-like electrons of arsenic atoms.

References

[1] De Franceschi S, Kouwenhoven L, Schönenberger Ch and Wernsdorfer W 2010 *Nat. Nanotech.* **5** 703
[2] Huefner M, May C, Kičin S, Ensslin K, Ihn T, Hilke M, Suter K, de Rooij N F and Staufer U 2009 *Phys. Rev. B* **79** 134530
[3] Wang Q Y, Li Z, Zhang W H, Zhang Z C, Zhang J S, Li W, Ding H, Ou Y B, Deng P, Chang K, Wen J, Song C L, He K, Jia J F, Ji S H, Wang Y Y, Wang L L, Chen X, Ma X C and Xue Q K 2012 *Chin. Phys. Lett.* **29** 037402
[4] Ge J F, Liu Z L, Liu C H, Gao C L, Qian D, Xue Q K, Liu Y and Jia J F 2015 *Nat. Mater.* **14** 285
[5] Hsu F C, Luo J Y, Yeh K W, Chen T K, Huang T W, Wu Pang Y L, Chu Y Y, Yan D C and Wu M K 2008 *Proc. Natl. Acad. Sci.* **105** 14262
[6] Lee J J, Schmitt F T, Moore R G, Johnston S, Cui Y T, Li W, Yi M, Liu Z K, Hashimoto M, Zhang Y, Lu D H, Devereaux T P, Lee D H and Shen Z X 2014 *Nature* **515** 245
[7] Uchoa B and Castro Neto A H 2007 *Phys. Rev. Lett.* **98** 146801
[8] Profeta G, Calandra M and Mauri F 2012 *Nat. Phys.* **8** 131
[9] Tiwari A P, Shin S, Hwang E, Jung S G, Park T and Lee H 2015 arXiv: 1508.06360
[10] Chapman J, Su Y, Howard C A, Kundys D, Grigorenko A, Guinea F, Geim A K, Grigorieva I V and Nair R R 2016 *Sci. Rep.* **6** 23254
[11] Si C, Liu Z, Duan W and Liu F 2013 *Phys. Rev. Lett.* **111** 196802
[12] Liu H, Neal A T, Zhu Z, Luo Z, Xu X, Tomáanek D and Ye P D 2014 *ACS Nano* **8** 4033
[13] Lalmi B, Oughaddou H, Enriquez H, Kara A, Vizzini S, Ealet B and Aufray B 2010 *Appl. Phys. Lett.* **97** 223109
[14] Chen L, Liu C C, Feng B, He X, Cheng P, Ding Z, Meng S, Yao Y and Wu K 2012 *Phys. Rev. Lett.* **109** 056804
[15] Mannix A J, Zhou X F, Kiraly B, Wood J D, Alducin D, Myers B D, Liu X L, Fisher B L, Santiago U, Guest J R, Yacaman M J, Ponce A, Oganov A R, Hersam M C and Guisinger N P 2015 *Science* **350** 1513
[16] Feng B, Zhang J, Zhong Q, Li W, Li S, Li H, Cheng P, Meng S, Chen L and Wu K 2016 *Nat. Chem.* **8** 563
[17] Chen L, Li H, Feng B, Ding Z, Qiu J, Cheng P, Wu K and Meng S 2013 *Phys. Rev. Lett.* **110** 085504
[18] Nie Y F, Brahimi E, Budnick J I, Hines W A, Jain M and Wells B O 2009 *Appl. Phys. Lett.* **94** 242505
[19] Ding F, Ji H, Chen Y, Herklotz A, Dörr K, Mei Y, Rastelli A and Schmidt O G 2010 *Nano Lett.* **10** 3453
[20] Conley H J, Wang B, Ziegler J I, Haglund Jr R F, Pantelides S T and Bolotin K I 2013 *Nano Lett.* **13** 3626
[21] Wan W, Ge Y, Yang F and Yao Y 2013 *Europhys. Lett.* **104** 36001
[22] Shao D F, Lu W J, Lv H Y and Sun Y P 2014 *Europhys. Lett.* **108** 67004
[23] Ge Y, Wan W, Yang F and Yao Y 2015 *New J. Phys.* **17** 035008
[24] Penev E S, Kutana A and Yakobson B I 2016 *Nano Lett.* **16** 2522
[25] Gao M, Li Q Z, Yan X W and Wang J 2017 *Phys. Rev. B* **95** 024505
[26] Cheng C, Sun J T, Liu H, Fu H X, J. Zhang, Chen X R and Meng S 2017 *2D Mater.* **4** 025032
[27] Zhang S, Yan Z, Li Y, Chen Z and Zeng H 2015 *Angew. Chem. Int. Ed.* **54** 3112
[28] Kamal C and Ezawa M 2015 *Phys. Rev. B* **91** 085423
[29] Pizzi G, Gibertini M, Dib E, Marzari N, Iannaccone G and Fiori G 2016 *Nat. Communs.* **7** 12585
[30] Zhang H, Ma Y and Chen Z 2015 *Nanoscale* **7** 19152

[31] Giannozzi P, Baroni S, Bonini N, et al. 2009 *J. Phys.: Condens. Matter* **21** 395502
[32] Troullier N and Martins J L 1991 *Phys. Rev. B* **43** 1993
[33] Giustino F, Cohen M L and Louie S G 2007 *Phys. Rev. B* **76** 165108
[34] Methfessel M and Paxton A T 1989 *Phys. Rev. B* **40** 3616
[35] Baroni S, De Gironcoli S, Dal Corso A and Giannozzi P 2001 *Rev. Mod. Phys.* **73** 515
[36] Marzari N and Vanderbilt D 1997 *Phys. Rev. B* **56** 12847
[37] Souza I, Marzari N and Vanderbilt D 2001 *Phys. Rev. B* **65** 035109
[38] Mostofi A A, Yates J R, Lee Y S, Souza I, Vanderbilt D and Marzari N 2008 *Comput. Phys. Commun.* **178** 685
[39] Mostofi A A, Yates J R, Pizzi G, Lee Y S, Souza I, Vanderbilt D and Marzari N 2014 *Comput. Phys. Commun.* **185** 2309
[40] Noffsinger J, Giustino F, Malone B D, Park C H, Louie S G and Cohen M L 2010 *Comput. Phys. Commun.* **181** 2140
[41] Poncáe S, Margine E R, Verdi C and Giustino F 2016 *Comput. Phys. Commun.* **209** 116
[42] Allen P B 1972 *Phys. Rev. B* **6** 2577
[43] Allen P B and Dynes R C 1975 *Phys. Rev. B* **12** 905
[44] Cahangirov S, Topsakal M, Aktürk E, Şahin H and Ciraci S 2009 *Phys. Rev. Lett.* **102** 236804
[45] Şahin H, Cahangirov S, Topsakal M, Bekaroglu E, Akturk E, Senger R T and Ciraci S 2009 *Phys. Rev. B* **80** 155453
[46] Tsai H S, Wang S W, Hsiao C H, Chen C W, Ouyang H, Chueh Y L, Kuo H C and Liang J H 2016 *Chem. Mater.* **28** 425
[47] Madelung O 2004 *Semiconductors: Data Handbook*, 3rd edn. (New York: Springer-Verlag) pp. 405–411, ISBN 3540404880
[48] Yuan H, Shimotani H, Tsukazaki A, Ohtomo A, Kawasaki M and Iwasa Y 2009 *Adv. Funct. Mater.* **19** 1046
[49] Fujimoto T and Awaga K 2013 *Phys. Chem. Chem. Phys.* **15** 8983